

Wave space sonification of the folding pathways of protein molecules modeled as hyper-redundant robotic mechanisms

Amal Kacem¹ · Khalil Zbiss¹ · Paul Watta¹ · Alireza Mohammadi¹

II. 🖱

Received: 19 October 2022 / Revised: 21 February 2023 / Accepted: 15 April 2023 © The Author(s), under exclusive licence to Springer Science+Business Media, LLC, part of Springer Nature 2023

Abstract

Investigation of the folding pathways of protein molecules plays a key role in studying diseases such as Alzheimer's and designing viral drugs at the molecular level. Despite recent advances in visualization techniques, effective sonification (i.e., non-speech auditory representation) of large datasets associated with protein folding pathways is still an open question. This paper investigates the problem of sonification of protein folding pathway datasets by using the wave space sonification (WSS) framework due to Hermann (2018). In particular, this paper utilizes the powerful WSS framework to develop a sonification methodology for the dihedral angle folding trajectories of protein molecules, which are modeled as hyper-redundant robotic mechanisms with many rigid nano-linkages. As an example, the developed sonification methodology is applied to a protein molecule backbone chain with a dihedral angle space of dimension 82, where a canonical wave space function based on a sum-of-sinusoids with conformation-dependent frequencies and a sample-based wave space function based on Mozart's Alla Turca are utilized for sonification of the folding trajectories of this peptide chain.

Keywords Sonification \cdot Protein folding \cdot Hyper-redundant robots \cdot Wave Space Sonification (WSS)

Amal Kacem and Khalil Zbiss contributed equally to this work.

> Amal Kacem akacem@umich.edu

Khalil Zbiss kzbiss@umich.edu

Paul Watta watta@umich.edu

Published online: 30 May 2023

Department Electrical & Computer Engineering, University of Michigan–Dearborn, 4901 Evergreen Rd., Dearborn, MI 48128, USA



1 Introduction

To execute a variety of important biological functions such as force generation in motor proteins and protein-ligand binding, protein molecules vary their three-dimensional structure between two or more native conformations through the processes of folding and unfolding [18]. Numerical algorithms, which can predict the structures of folded protein molecules and the pathways/transitions through which proteins fold/unfold, have an integral role in computer-aided drug discovery [7] and designing protein-based nanomachines [12, 46].

Despite their high computational burden, physics-based approaches relying on physical first principles are still the more preferred way to numerically compute the protein folding pathways [41]. To address the high computational times associated with the approaches relying on physical first principles, the computationally efficient framework of kinetostatic compliance method (KCM), pioneered by Kazerounian, Ilieş, and collaborators, models protein molecules as nano-linkage-based mechanisms that form a hyper-redundant robot, which fold under the nonlinear effect of interatomic forces [6, 39, 53, 55]. Since its advent, the KCM framework has been successfully applied to studying the formation of hydrogen bonds and their impact on protein kinematic mobility [51] and design of peptide-based molecular nano-linkages [12]. Furthermore, using nonlinear optimization-based control algorithms, it has been shown that entropy-loss constraints during protein folding (see, e.g., [52] for the importance of these constraints) can be encoded in the KCM framework [43]. Finally, Chetaev instability analysis can be utilized for synthesizing unfolding control inputs (e.g., computing proper optical tweezer forces for unfolding in desired directions) for the KCM-based model of protein molecules [44].

Numerical simulation of protein folding for computing the molecule conformational changes generates an *overwhelming amount of data*. Accordingly, one is still left with the problem of representing these large folding pathway datasets. Despite the recent advent of visualization techniques developed for representing the protein folding pathway datasets (see, e.g., [17]), their sonification, where non-speech audio is utilized for conveying information, has remained an unaddressed question.

In this paper, we employ the recent *Wave Space Sonification (WSS)* paradigm due to Hermann [28] to answer the challenging question of generating *non-speech auditory representation* of large datasets associated with protein folding pathways (see Fig. 1). WSS is a class of sonification techniques developed for high-dimensional data (indexed by time or space), which relies on generating an auditory data representation by scanning a scalar field along a data-driven trajectory of interest. In this paper, we demonstrate that WSS provides a novel approach for creating non-speech auditory representations of protein folding pathway datasets through a data-driven audio signal sampling, which is afforded by a high-dimensional scalar sound field defined on the dihedral angle space of protein conformations.

Contributions of the paper The contributions of this paper are described in what follows. First, despite the innovative application of numerous sonification techniques to the problem of translating protein structural/vibrational data to musical compositions (see, e.g., [19, 20, 49, 60, 61]), the problem of folding pathway sonification is still an open problem. This article, relying on the WSS framework, provides a solution to this problem for the first time. Our non-speech auditory representation framework for protein folding processes complements the recent line of work by Ferina and Daggett for visualization of folding [17]. Second, this paper contributes to the field of robotic trajectory sonification, which is still in its early development stages. Despite the application of sonification techniques to several



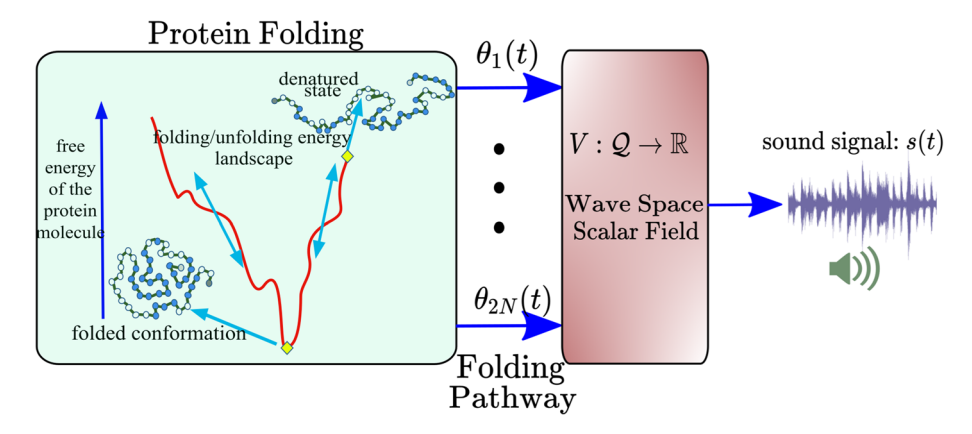


Fig. 1 A novel WSS-based technique for creating non-speech auditory representations of protein folding pathway datasets is proposed. Such a sonification is achieved through a data-driven audio signal sampling, which is afforded by a high-dimensional scalar sound field defined on the dihedral angle space of protein conformations

human-robot interaction (HRI) problems [22, 48, 58], the problem of sonification of joint space trajectories for robots with many degrees-of-freedom has remained unaddressed. The proposed sonification methodology in this paper paves the path for sonification of robotic trajectories in other contexts such as soft robotics [24, 59] and industrial collaborative multirobot systems [16, 23, 62], where the robotic system operation generates an overwhelming amount of motion data. Further details are provided in Remarks 1–3 in Section 2, where we highlight the contributions of the paper in the context of existing literature.

The paper organization can be described as follows. After presenting the necessary background on sonification, its state-of-the-art applications in robotics, and sonification of protein-related data in Section 2, we provide a brief overview of KCM-based protein folding and its relationship to robotics in Section 3. Thereafter, in Section 4, we provide our solution to the problem of sonification of datasets associated with conformational changes of protein molecules during folding. Next, in Section 5, we apply our developed WSS-based methodology to the backbone chain of a protein molecule with a conformation vector of dimension 82. Specifically, we utilize a canonical wave space function based on a sum-of-sinusoids with protein conformation-dependent frequencies and a sample-based wave space function based on Mozart's Alla Turca for sonification of the peptide chain folding trajectories. Finally, in Section 6, we discuss the significance of our proposed solution in the context of sonification of motion of other hyper-redundant robots as well as further remarks and future research directions.

Notation Given the real vector $\mathbf{x} \in \mathbb{R}^M$, we denote the Euclidean and the maximum norms of the vector by $|\mathbf{x}| := \sqrt{\mathbf{x}^\top \mathbf{x}}$ and $|\mathbf{x}|_{\infty} := \max_{1 \le i \le M} |x_i|$, respectively. Given a function $f: U \to V$ with domain U and codomain V, we let $f: u \mapsto v$ denote f(u) = v for all $u \in U$ and $v = f(u) \in V$. Finally, by $f(\cdot)$, we mean that f is a function without identifying its domain and codomain.

¹The generated sound files (in .wav format) based on our WSS-based proposed method can be downloaded from https://dralirezamoha.github.io/proteinpathway/wssFoldingSoundFiles.zip. See Section 5 for further details.



2 Background

We briefly review the background on sonification techniques and their applications to datasets resulting from studying protein molecules as well as robotic motion sonification. We further highlight the contributions of this paper with respect to the recent sonification techniques applied to these important problems in Remarks 1–3.

2.1 Sonification

Sound, from René Laennec's stethoscope to Geiger-Müller counter, has had a longstanding importance in the process of scientific discovery and technological development [57]. Despite this significance, the utilization of non-speech audio for conveying information, which is known as **sonification**, is still at its developing phase (see, e.g., [5, 29, 47]). Formally, sonification can be defined as the technique of using datasets as input and generating sound signals as output, while satisfying the four conditions of: (i) reflecting the objective and/or relational properties in the input data; (ii) transforming datasets systematically; (iii) being reproducible; and, (iv) being applicable to versatile datasets [31].

The Sonification Handbook [31] categorizes (see, also, [27]) the sonification techniques to five different structural classes, namely, earcons, auditory icons, parameter-mapping sonification, audification, and model-based sonification. Earcons refer to structured sounds serving as an index for abstract messages, such as the Windows abstract operating system sounds or the signature three-tone melody of the National Broadcasting Company (NBC). Auditory icons refer to short sound messages that convey information about an event, situation, or object [11] (see, also, [8]) such as the crumpling sound of a paper piece during a document deletion in Windows. Audification is a special case of WSS where data is directly translated into sound. Finally, in model-based sonification [30], the dataset is converted to a dynamical system that demonstrates acoustic behavior, e.g., utilizing the data to determine the mass-spring system parameters of an acoustic device.

In addition to the five established classes of sonification, a new class known as the wave space sonification (WSS) has been recently proposed by Hermann [28]. This framework lies in the spectrum between parameter-mapping sonification and audification. WSS, whose essence is based on effective navigation of sound signal spaces by using high-dimensional data, has been utilized in few applications such as development of audiovisual dance displays [34].

Remark 1 In this paper, we utilize the WSS framework for solving the problem of sonification of dihedral angle folding trajectories of protein molecules, which are modeled as hyper-redundant robotic mechanisms (see, e.g., the line of work in [25, 36, 56] for such a robot kinematics-based point of view on the structure of proteins). This is the first time that Hermann's WSS framework [28] is utilized for navigating sound signal spaces by using high-dimensional data resulting from the folding process of protein molecules.

2.2 Sonification techniques applied to structural/vibrational protein data

One of the very first endeavors to sonify the structure of proteins and their encoding gene sequences is due to Dunn and Clark [14]. In their work, fixed pitches were assigned to each amino acid based on an absolute basis or more consonant intervals were assigned to the more frequently occurring amino acids based on a relative basis. Furthermore, water solubility of amino acids was also considered as a third metric for pitch assignment. Another pioneering



work on molecular data sonification is due to Delatour [13], where a conversion process for the musical and acoustic vibrational spectra data was proposed.

Following Dunn and Clark [14] and Delatour [13], many of the important methods in this area such as the innovative line of work by Buehler and collaborators [19, 20, 49, 60, 61] fall within translation of either structural properties or vibrational spectra of proteins into sound/musical compositions. Of notable importance is the work by Franjou *et al.* [19] where a neural network model is trained on 'protein music' and gives rise to new musical structures. These novel musical compositions, in turn, can be utilized to generate new protein structures through proper translation mappings. In another notable work, Qin and Buehler [49] employ frequency spectra of proteins, which result from a high-throughput automatic computational method, to produce audible sound. Moreover, using the concept of transpositional equivalence in music theory, they overlay the vibration of molecular structures and translate them to the audible frequency range (see [49] for further details).

Remark 2 Despite all the previous development for sonification of protein molecule structural/vibrational data, the problem of sonification of protein folding pathway datasets is still an open one. This challenge is mainly due to the existence of an overwhelming amount of data, which are generated using physics-based numerical simulations (see, e.g., [17, 55]), associated with time-indexed dihedral angle trajectories. Indeed, it is not clear how one can assign sound/music signals to these trajectories lying in the high-dimensional conformation space of protein molecules.

2.3 Sonification of robotic motion/gestures

Sonification of the motion of robots is a relatively new paradigm with many potentials for efficient communication of robotic motion/intentions to human users while relying less on visual engagement [9, 10, 21, 22, 48, 50, 58, 63]. A notable approach, which belongs to the family of Parameter Mapping Sonification methods, is proposed by Schwenk *et al.* [50]. In their approach, a robot sonification system based on sound modulation of a synthesizer has been developed, where joint state and sensor data are fed into the synthesizer.

Another notable line of work is the SONAO project led by Frid, Bresin, and collaborators [10, 21, 22], where communicative channel impediments in robot interaction with humans are compensated through mapping humanoid robot expressive gestures to nonspeech audio. For instance, Frid and Bresin [21] used a rectangular oscillator with an envelope of short time span while transforming the input magnitude to C major scale pitches to convey sensations of joy.

In the context of virtual reality-based robot teleoperation, Bremner *et al.* [9] have decreased the stress and perceived workload of human operators working with remote robots in hazardous environments by using proper data sonification through the Parameter Mapping Sonification framework. Another relevant project is SonifyIt [63] that enables sample playback and live sound synthesis for robots using Robot Operating System (ROS) and a visual programming language for multimedia called Pure Data.

Remark 3 Despite the advancements in the field of robot motion sonification, one major limitation of the recent methods is that they are limited to robotic systems with a configuration space of low dimensionality (e.g., less than ten degrees-of-freedom like the robot Daryl in [50]). On the other hand, hyper-redundant robots such as elephant trunk robotic arms or segmented space manipulators (see, e.g., [32, 40, 64]), which can efficiently operate within constrained environments or executing novel types of locomotive patterns, have



a huge or infinite number of degrees-of-freedom. The KCM approach [35, 36, 55] for protein molecules also relies on modeling the proteins as hyper-redundant robotic mechanisms with each dihedral angle corresponding to one degree-of-freedom of the mechanism (see Section 3 for further details). Furthermore, each dihedral angle trajectory is a time series generated by the protein folding dynamical model. For instance, the backbone chain of the protein Triponin with 159 amino acids has 320 dihedral angles that change with time during the Triponin folding process. Consequently, Triponin folding results in 320 time-indexed trajectories. For the first time, we provide a systematic way of sonifying the high-dimensional data resulting from the motion of protein molecules that are modeled as hyper-redundant robotic mechanisms.

3 Kinetostatic Compliance-based protein folding

We briefly present some background on the Kinetostatic Compliance Method (KCM) for modeling of the folding of protein molecules *in vacuo*. We limit our presentation to the protein main chain for brevity.

3.1 Nano-linkage-based kinematic model of protein molecules

Protein molecules consist of many peptide planes that are connected together through chemical bonds to form long molecular chains, where each plane consists of six coplanar atoms. As demonstrated in Fig. 2, these planes can be considered as the linkages of the protein kinematic mechanism [36, 56]. Central carbon atoms, which are also known as the alpha-Carbon atoms denoted by C_{α} , function as inter-peptide plane hinges. Indeed, C_{α} atoms in protein molecules can be considered as the revolute joints in this kinematic mechanism. The line segments colored in red in Fig. 2 are the interatomic covalent chemical bonds in the peptide plane.

Remark 4 The assumption of the six atoms $C_{\alpha} - CO - NH - C_{\alpha}$ being coplanar, which constitute each of the peptide planes (see Fig. 2), is based on the high resolution X-ray crystallographic experimentally validated observations of the protein molecule structures (see, e.g., [18]). This coplanarity assumption has been the basis of various robotics-inspired

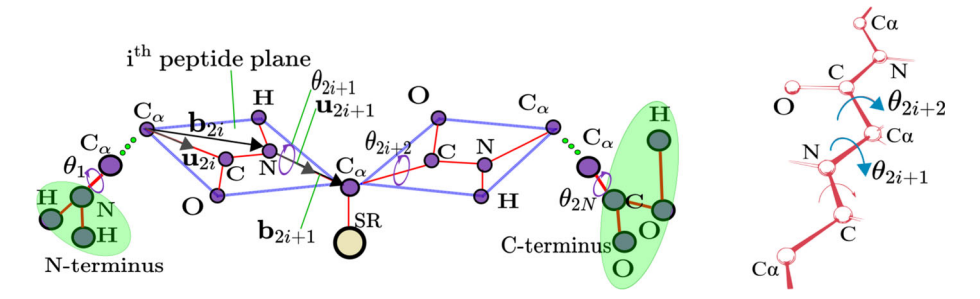


Fig. 2 (Left) The protein molecule kinematic structure consisting of peptide planes (similar to robotic linkages) and C_{α} atom hinges (similar to robotic revolute joints). There also exists a hydrogen atom that is bonded to each alpha-Carbon atom using a covalent chemical bond but not shown in the figure. (Right) The dihedral angles



approaches in the literature that model protein molecules as hyper-redundant mechanisms (see, e.g., [25, 55]).

As it is demonstrated in Fig. 2, each individual C_{α} is bonded to four other components, namely, a side chain of variable structure denoted by SR and the three atoms C, N, and H. The first C_{α} of the protein chain structure is connected to N-terminus, which is an amino group, as well as one other peptide plane. Finally, the last alpha-Carbon atom gets connected to the C-terminus, which is a carboxyl group, as well as one other peptide plane.

The backbone conformation² of the protein molecule kinematic structure formed by $-N-C_{\alpha}-C-$ atoms, is fully described by a collection of bond lengths as well as a collection of pairs of dihedral angles, namely, the rotation angles about the bond connecting C_{α} to -C and the bond connecting N to C_{α} . A protein molecule dihedral angle can be defined as the internal angle of the polypeptide backbone at which two adjacent planes meet (i.e., at each C_{α} atom). Therefore, the backbone conformation can be represented by two dihedral angles per residue, because the backbone residing between two juxtaposing alpha-Carbon atoms are all in a single plane (see Fig. 2). Accordingly,

$$\boldsymbol{\theta} := [\theta_1, \cdots, \theta_{2N}]^{\top} \in \mathcal{Q}, \tag{1}$$

is the configuration vector of the kinematic structure of a given protein backbone chain possessing N-1 peptide planes. As indicated by (1), the dihedral angle vector $\boldsymbol{\theta}$ belongs to the 2N-dimensional configuration space $\mathcal{Q} := \mathcal{S}^1 \times \cdots \times \mathcal{S}^1$, where \mathcal{S}^1 is the unit circle.

Each of the dihedral angles in the conformation vector $\boldsymbol{\theta}$ in (1) correspond to one degree-of-freedom (DOF) of the protein molecule kinematic chain. Associated with each DOF, one may consider a direction vector of unit length denoted by \mathbf{u}_j , $1 \le j \le 2N$. Each of these unit vectors are aligned with the rotation axis about which the protein kinematic chain can rotate. Therefore, as demonstrated in Fig. 2, the unit vectors \mathbf{u}_{2i} and \mathbf{u}_{2i+1} are aligned with the $C_{\alpha} - C$ and $N - C_{\alpha}$ bonds of the *i*-th peptide plane, respectively. Finally, \mathbf{u}_1 and \mathbf{u}_{2N} are the unit vectors associated with the N- (the amino group) and C-termini (the carboxyl group), respectively.

Along with the unit vectors \mathbf{u}_j , one may utilize another collection vectors, which are known as the **body vectors**, to fully determine the three-dimensional orientation of the rigid peptide nano-linkages in protein molecules. The body vectors, which are denoted by \mathbf{b}_j , $1 \le j \le 2N$, fully describe the relative position of any two coplanar peptide plane atoms. Specifically, the relative position vector connecting any two atoms is determined by combining the body vectors through a linear sum of the form $k_{1m}\mathbf{b}_{2i} + k_{2m}\mathbf{b}_{2i+1}$, in which the coefficients k_{1m} and k_{2m} , $1 \le m \le 4$, are constant and the same across all peptide linkages (see, e.g., [2, 54] for more elaborations).

The unit vectors \mathbf{u}_j and the body vectors \mathbf{b}_j can be utilized for complete description of the molecule conformation by utilizing the conformation vector $\boldsymbol{\theta}$ consisting of the peptide dihedral angles. Indeed, after choosing the zero position configuration as $\boldsymbol{\theta} = \mathbf{0}$, the rotational transformations

$$\mathbf{u}_{j}(\boldsymbol{\theta}) = \Xi(\boldsymbol{\theta}, \mathbf{u}_{j}^{0})\mathbf{u}_{j}^{0}, \ \mathbf{b}_{j}(\boldsymbol{\theta}) = \Xi(\boldsymbol{\theta}, \mathbf{u}_{j}^{0})\mathbf{b}_{j}^{0}, \tag{2}$$

²In the biochemistry literature, 'conformation' is the standard word for describing the geometric structure of a protein molecule. In the robotics literature, on the other hand, the terminology 'configuration' is frequently used to describe the kinematic structures of robots. In this paper, unless otherwise stated, we use the two words 'conformation' and 'configuration' interchangeably.



where the transformation matrix is $\Xi(\pmb{\theta}, \mathbf{u}_j^0)$ defined according to

$$\Xi(\boldsymbol{\theta}, \mathbf{u}_j^0) := \prod_{r=1}^j R(\theta_j, \mathbf{u}_j^0), \tag{3}$$

where the superscript 0 indicates the reference zero position (ZP) conformation. The zero position conformation of the protein molecule refers to a linear structure in which all the amino acid peptide nano-linkages lie on the same plane (i.e., a completely stretched protein chain with dihedral angle vector $\boldsymbol{\theta} = \mathbf{0}$). Therefore, using the ZP conformation, we are expressing all the possible directions of the unit vectors \mathbf{u}_j and body vectors \mathbf{b}_j in terms of rotational transformations applied to these vectors at the zero conformation where the protein chain is completely stretched.

The matrix $\Xi(\theta, \mathbf{u}_j^0)$ determines the molecule kinematic structure using the dihedral angle conformation vector $\boldsymbol{\theta}$. In (2), the rotation matrix $R(\theta_j, \mathbf{u}_j^0) \in SO(3)$ describes the rotation about the direction given by the unit vector \mathbf{u}_j^0 with an angle equal to θ_j . It is remarked that the special orthogonal group SO(3) is the set of all rotational matrices about the origin of three-dimensional Euclidean space. Furthermore, any rotation matrix $R(\alpha, \hat{\mathbf{v}})$, where α is an angle and $\hat{\mathbf{v}} = [\hat{v}_x, \hat{v}_y, \hat{v}_z]^{\mathsf{T}}$ is a unit vector, can be written as

$$R(\alpha, \hat{\mathbf{v}}) = \begin{bmatrix} \hat{v}_x^2 V_\alpha + C_\alpha & \hat{v}_x \hat{v}_y V_\alpha - \hat{v}_z S_\alpha & \hat{v}_x \hat{v}_z V_\alpha + \hat{v}_y S_\alpha \\ \hat{v}_x \hat{v}_y V_\alpha + \hat{v}_z S_\alpha & \hat{v}_y^2 V_\alpha + C_\alpha & \hat{v}_y \hat{v}_z V_\alpha - \hat{v}_x S_\alpha \\ \hat{v}_x \hat{v}_z V_\alpha - \hat{v}_y S_\alpha & \hat{v}_y \hat{v}_z V_\alpha + \hat{v}_x S_\alpha & \hat{v}_z^2 V_\alpha + C_\alpha \end{bmatrix},$$
(4)

where $V_{\alpha} := 1 - \cos(\alpha)$, $C_{\alpha} := \cos(\alpha)$, and $S_{\alpha} := \sin(\alpha)$.

After the body vectors $\mathbf{b}_{j}(\boldsymbol{\theta})$ are determined from (2) and assuming that the N-terminus atom is located at the origin, the position vectors of the atoms belonging to the backbone chain, which are located in the k^{th} -peptide plane, are computed from

$$\mathbf{r}_{i}(\boldsymbol{\theta}) = \sum_{i=1}^{i} \mathbf{b}_{j}(\boldsymbol{\theta}), \quad 1 \le i \le 2N - 1,$$
(5)

where the indices i = 2k - 1 and i = 2k are associated with the N and alpha-Carbon atoms, respectively.

Remark 5 The zero position for the conformation of the protein molecule refers to a linear structure in which all the amino acid peptide nano-linkages lie on the same plane (i.e., a completely stretched protein chain with dihedral angle vector $\boldsymbol{\theta} = \mathbf{0} \in \mathbb{R}^{2N}$). On the other hand, the zero position for the N-terminus nitrogen atom means that this atom is treated as the fixed base of the mechanism located at $[0, 0, 0]^T$. The reason for fixing the position of the N-terminus nitrogen atom at the origin is that it is only the changes in the conformation vector of the protein molecule that results in changes of the three-dimensional structure of the molecule independent of the choice of the N-terminus nitrogen atom base position.

3.2 Folding according to the KCM iteration

The KCM approach for modeling the protein folding process pioneered by Kazerounian and collaborators is based on the experimental fact that the inertial forces can be neglected in the folding process (see, e.g., [1, 3, 4, 35]). Instead, the protein chain dihedral angles vary under the kinetostatic influence of the van der Waals and electrostatic interatomic forces in the protein molecules. Consequently, in the KCM framework, the dihedral angle variation



about the alpha-Carbon atoms at each molecule individual conformation is proportional to the effective torques acting on the peptide chain.

Considering a peptide chain with N_a atoms and N-1 peptide planes with the configuration vector $\boldsymbol{\theta} \in \mathcal{Q}$ and denoting the Cartesian position of any two single atoms a_i , a_j belonging to the molecule chain by $r_i(\boldsymbol{\theta})$, $r_j(\boldsymbol{\theta})$, their distance can be computed from $d_{ij}(\boldsymbol{\theta}) := |r_i(\boldsymbol{\theta}) - r_j(\boldsymbol{\theta})|$. It is remarked that the number of atoms in the main backbone chain of the protein molecule (ignoring the side chains and the individual hydrogen atoms connected to alpha-Carbon atoms which are not in the peptide planes) is equal to $N_a = 5N + 8$, where the added constant take into account the number of atoms in the N-terminus and C-terminus.

Furthermore, we denote the respective electrostatic charges of a_i , a_j by q_i , q_j , their van der Waals radii by R_i , R_j , their van der Waals distance by $D_{ij} = R_i + R_j$, their dielectric constant by ε_{ij} , and their potential well depth as ϵ_{ij} . Finally, we let $w_{ij}^{\rm elec}$ and $w_{ij}^{\rm vdw}$ represent the weight factors for the electrostatic and van der Waals forces between the two atoms a_i and a_j , respectively. All of these parameters are provided in [54] and its references. Under these considerations, the molecule aggregated free energy can be computed from

$$\mathscr{G}(\boldsymbol{\theta}) := \mathscr{G}^{\text{elec}}(\boldsymbol{\theta}) + \mathscr{G}^{\text{vdw}}(\boldsymbol{\theta}), \tag{6}$$

where

$$\mathscr{G}^{\text{elec}}(\boldsymbol{\theta}) = \sum_{i=1}^{N_a} \sum_{j \neq i} \frac{w_{ij}^{\text{elec}}}{4\pi \varepsilon_{ij}} \frac{q_i q_j}{d_{ij}(\boldsymbol{\theta})},\tag{7}$$

is the molecule potential energy resulting from the interatomic electrostatic interactions, and

$$\mathscr{G}^{\text{vdw}}(\boldsymbol{\theta}) = \sum_{i=1}^{N_a} \sum_{j \neq i} w_{ij}^{\text{vdw}} \epsilon_{ij} \left[\left(\frac{D_{ij}}{d_{ij}(\boldsymbol{\theta})} \right)^{12} - 2 \left(\frac{D_{ij}}{d_{ij}(\boldsymbol{\theta})} \right)^{6} \right]$$
(8)

is the molecule potential energy due to the van der Waals interactions. The resultant Coulombic and van der Waals forces on each atom a_i , $1 \le i \le N_a$, can be computed from $F_i^{\text{elec}}(\boldsymbol{\theta}) = -\nabla_{\mathbf{r}_i} \mathcal{G}^{\text{elec}}$ and $F_i^{\text{vdw}}(\boldsymbol{\theta}) = -\nabla_{\mathbf{r}_i} \mathcal{G}^{\text{vdw}}$, respectively. It is remarked that $\nabla_{\mathbf{r}_i} \mathcal{G}^j$, where j = elec or j = vdw, is the gradient of the potential function \mathcal{G}^j with respect to the position vector \mathbf{r}_i .

The KCM-based folding process is performed according to a successive numerical iteration up to the moment that all of the kinetostatic torques converge to a local minimum on the aggregated free energy landscape. To perform this numerical iteration, one can compute the effective forces and torques acting on each of the N-1 peptide planes, which are the rigid nano-linkages of the protein kinematic mechanism, and appending them in the generalized force $\mathscr{F}(\theta) \in \mathbb{R}^{6N}$. Using a proper mapping, it is possible to map the generalized force $\mathscr{F}(\theta)$ to the equivalent torque vector influencing the configuration vector θ . Specifically, the vector $\tau(\theta) \in \mathbb{R}^{2N}$, which is the overall joint torques resulting from the interatomic forces in the protein kinematic structure, can be computed according to

$$\tau(\boldsymbol{\theta}) = \boldsymbol{\mathcal{J}}^{\top}(\boldsymbol{\theta})\boldsymbol{\mathcal{F}}(\boldsymbol{\theta}),\tag{9}$$

where the Jacobian matrix $\mathscr{J}(\theta) \in \mathbb{R}^{6N \times 2N}$ is the determined by the kinematic structure of the protein chain at conformation θ (see [35, 55] for the calculation details). It is remarked that the vector $\mathscr{F}(\theta)$ is generated by the torques and forces acting on the peptide planes at each conformation vector θ .

³The dissertation can be accessed and downloaded by the public through the URL address https://opencommons.uconn.edu/dissertations/1024/.



Starting from the initial unfolded conformation θ_0 , the difference equation

KCM Iteration:
$$\theta_{k+1} = \theta_k + \frac{h}{|\tau(\theta_k)|_{\infty}} \tau(\theta_k),$$
 (10)

describes the KCM-based numerical iteration due to Kazerounian and his collaborators, where the non-negative integer k determines the iteration number and h is a positive real constant equal to the maximum magnitude of the dihedral angle rotation in each step.

Starting from an unfolded conformation, the KCM iteration in (10) gives rise to the protein folding pathway data. In particular, the protein molecule backbone *folding pathway* trajectory is the dihedral angle vector series $\{\theta_k\}_{k=0}^{N_s}$, with $\theta_u := \theta_0$ corresponding to the initial unfolded conformation and $\theta_f := \theta_{N_s}$ corresponding to the final folded conformation. The KCM framework also renders itself to control input synthesis interpretations. For instance, it has been shown in [43] that entropy-loss constraints during protein folding can

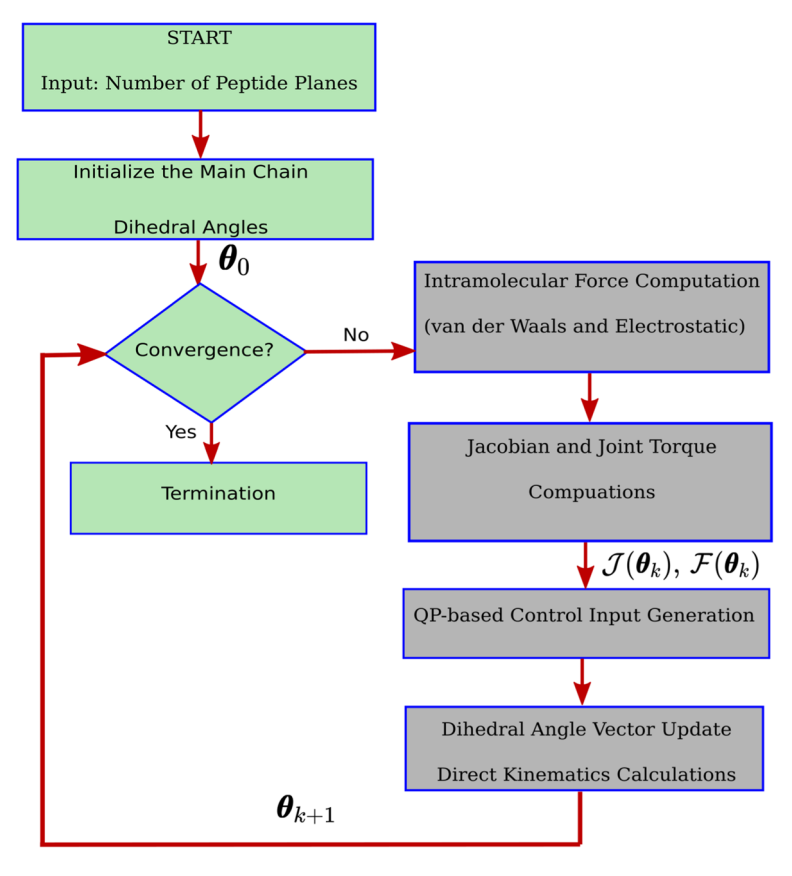


Fig. 3 The flow chart associated with the KCM iteration with entropy-loss constraints encoded in the protein folding process (see [43] for further details). Such iterative KCM-based numerical algorithms give rise to the protein folding pathway datasets. The objective of this paper is the sonification of such folding pathway dihedral angle trajectories. It is remarked that the convergence criterion is based on checking the norm of the generalized protein folding force vector $\mathscr{F}(\theta)$. If the initial conformation θ_0 happens to be a folded conformation, then $\mathscr{F}(\theta_0) = \mathbf{0}$, and there is no need for performing the iterations. However, if the initial conformation θ_0 is an unfolded conformation, then the KCM calculations need to be carried out until convergence of the norm of $\mathscr{F}(\theta)$ to a predetermined vicinity of zero



be encoded in the KCM framework using nonlinear optimization-based control algorithms (see the flow chart in Fig. 3).

In this paper we consider the time series associated with the dihedral angle vector folding pathway generated by the robotics-based KCM numerical iteration in (10) or its variations (see, e.g., [43, 44]). The dihedral angle pathway datasets can also be generated by other means such as all-atom molecular dynamics simulations, e.g., GROMACS [38]. The sonification methodology proposed in this paper can also be applied to such pathway datasets.

4 Wave space sonification of the folding pathways of protein molecules

In this section we provide our solution to the problem of sonification of datasets associated with conformational changes of protein molecules during folding. Our solution to this problem is based on the Wave Space Sonification (WSS) framework due to Hermann [28]. After providing the problem statement and the formal definition of WSS, we elaborate on the three WSS elements needed in the context of protein folding. Next, we present two WSS-based solutions to this problem, namely, canonical WSS and sample-based WSS in Sections 4.1 and 4.2, respectively.

Problem statement Consider a protein molecule with a backbone chain consisting of N-1 peptide planes modeled as a hyper-redundant robotic mechanism (see Section 3.1 for such a robotics-inspired modeling approach). Consider the protein molecule backbone folding pathway trajectory, namely, the dihedral angle vector time-indexed trajectory $\boldsymbol{\theta}(t)$, with $\boldsymbol{\theta}_u := \boldsymbol{\theta}(0)$ corresponding to the initial unfolded conformation and $\boldsymbol{\theta}_f := \boldsymbol{\theta}(T_f)$ corresponding to the final folded conformation. Find a non-speech auditory representation of the folding pathway trajectory given by $\boldsymbol{\theta}(\cdot)$.

WSS elements The WSS framework requires defining the following *three elements* [28]: (i) a trajectory in the *wave space*; (ii) a suitable definition of a *wave space function*; and, (iii) a *proper way of moving along the trajectory* in the wave space.

In the context of sonification of folding pathways of protein molecules, the wave space is the configuration space \mathcal{Q} to which the vector of dihedral angles belongs (see (1)). Furthermore, the dihedral angle vector trajectory $\boldsymbol{\theta}(t)$ obtained from the protein folding process defines an embedded trajectory within the high-dimensional wave space \mathcal{Q} . Moreover, in the WSS framework, one needs to select a morphing function $M:t\mapsto M(t)$, which determines how the dihedral angle folding trajectory is traversed. Finally, one needs to construct a scalar field $V:\mathcal{Q}\to\mathbb{R}$, which is also known as the *wave space function* (see, also, Fig. 1). After determining the wave space function $V(\cdot)$ (see Sections 4.1 and 4.2), the sound signal, which can be sent to the PC sound card for listening to the folding pathway, is given by

$$s(t) = V(\boldsymbol{\theta}(M(t))). \tag{11}$$

Figure 1 depicts the WSS elements in the context of sonification of protein folding pathway datasets. In the figure, the morphing function is considered to be the identity mapping, i.e., M(t) = t.



4.1 Solution based on canonical wave space sonification

In this section we present a canonical WSS-based scalar field for solving the stated sonification problem in Section 4. Canonical wave space functions, according to Hermann [28], are explicit algebraic expressions that utilize the data-driven trajectory under study for embedding in the wave space. In our context, these trajectories are given by time-indexed vectors of the form $\theta(t)$, which are the dihedral angle vector folding pathway trajectories.

For solving the sonification problem using the *canonical WSS approach*, we utilize a canonical wave space function $V_e: \mathcal{Q} \to \mathbb{R}$, which is a sum-of-sinusoids with conformation-dependent frequencies. In particular, we let

$$V_{c}(\boldsymbol{\theta}) := \frac{A_0}{2N} \sum_{i=1}^{2N} \sin\left(2\pi f_0 h(\boldsymbol{\theta}) \,\theta_i\right),\tag{12}$$

where the positive constant f_0 represents a desired base frequency, A_0 is a positive design parameter, and

$$h(\boldsymbol{\theta}) = \exp\left(\frac{-\|\boldsymbol{\theta} - \boldsymbol{\theta}_f\|}{\sigma_0^2 \|\boldsymbol{\theta}_u - \boldsymbol{\theta}_f\|}\right),\tag{13}$$

is a frequency weighting function, where $\sigma_0 \in (0, 1)$ is some positive constant less than one. We are using an exponential frequency resolution function $h(\theta)$ given by (13) because of the logarithmic nature of the way that the human auditory system perceives sounds (see, e.g., [15] for further information on how humans perceive sound). Indeed, two pure-tone sounds, which slightly differ from each other in their frequencies are not heard as separate notes by a single human ear. Since we are interested in making the listener to clearly perceive the protein folding process from an unfolded conformation to a folded one, such an exponential frequency resolution function is utilized within the proposed wave space function.

The significance of the proposed canonical wave space function in (12) and (13) is the generation of sounds with conformation-dependent frequencies. In particular, as the protein conformation approaches the final folded configuration θ_f from its unfolded initial conformation θ_u , sounds with higher frequency contents will be generated. The only design parameters for controlling the canonical wave space function in (12) and (13) are the base frequency f_0 and the parameter σ_0 . To generate a sound file of duration T_s from a folding pathway of time duration T_f , we use the linear morphing function $M(t) = \frac{T_f}{T_s}t$. Therefore, the generated sound signal takes the following form

$$s(t) = \frac{A_0}{2N} \sum_{i=1}^{2N} \sin\left(2\pi f_0 h\left(\theta\left(\frac{T_f}{T_s}t\right)\right) \theta_i\left(\frac{T_f}{T_s}t\right)\right). \tag{14}$$

Remark 6 (Comparison with the Original Canonical WSS) In Hermann's original work [28], the canonical wave space functions, which are written as sums-of-sinusoids, do not depend on the function $h(\theta)$ (or, equivalently, $h(\theta) = 1$ in Hermann's work). In this work, we are introducing the novel element of dependency of frequency components on the distance to desired locations in the dataset (here, folded and unfolded conformations of protein molecules). From this perspective, our proposed wave space function in (12) and (13) can also be viewed as a hybrid of Hermann's canonical wave space function (because of being written in terms of algebraic functions) and of Hermann's data-driven localized wave space function (because of dependency on designated points in a given dataset).



Remark 7 (Relationship to MIDI Applications) In Musical Instrument Digital Interface (MIDI) applications, the dihedral angle vectors $\boldsymbol{\theta}$, as well as the function $h(\boldsymbol{\theta})$ can be used as control signals (CC messages) to create amplitude envelopes and/or envelopes to control low frequency oscillators. Programs like CSound (see, e.g., [37]) or Cycling'74 Max⁴ are well suited for exploring these types of creative uses of the underlying data in a musical context. Though an additive-like synthesis was used in this paper (see (14)), other possible applications would be using the data as control parameters for other types of sound synthesis methods, such as frequency modulation (FM synthesis) and granular methods.

4.2 Sample-based wave space sonification solution

In this section we present a sample-based WSS scalar field for solving the stated sonification problem in Section 4. The *key idea* behind sample-based scalar fields is that instead of merely relying on mathematical functions as in their canonical counterparts in Section 4.1, one can define the wave space function through available samples from recorded sound signals [28]. Indeed, this point of view on wave space functions is motivated by the desire to generate acoustically more artistic and appealing sounds.

In the context of protein folding, datasets are given by time-indexed vectors of the form $\theta(t)$, which are the trajectories of the dihedral angle vector obtained from the folding process. For solving the sonification problem using the *sample-based WSS approach*, we utilize a sample-based wave space function $V_s: \mathcal{Q} \to \mathbb{R}$, which relies on recorded sounds, e.g., pieces of classical music. In particular, considering the collection of sound files $f_i: t \mapsto f_i(t), 1 \le i \le 2N$, we let

$$V_{s}(\boldsymbol{\theta}) := \frac{1}{2N} \sum_{i=1}^{2N} \mathcal{A}(c_{i}(\boldsymbol{\theta})), \tag{15}$$

where $c_i : \mathcal{Q} \to \mathbb{R}$, $1 \le i \le 2N$, are nonlinear scaling functions. In this article, we let these mappings to have the conformation-dependent form

$$c_i(\boldsymbol{\theta}) := \alpha_i \left\{ \lambda_{0,i} \exp\left(\frac{-\|\boldsymbol{\theta} - \boldsymbol{\theta}_f\|}{\sigma_{0,i}^2 \|\boldsymbol{\theta}_u - \boldsymbol{\theta}_f\|}\right) + \beta_i \right\}, \tag{16}$$

where $\lambda_{0,i}$ and $\sigma_{0,i}$ are some positive constants to be chosen by the sound designer. Having selected the design parameters $\lambda_{0,i}$ and $\sigma_{0,i}$, the constants α_i and β_i are given by

$$\beta_i = -\lambda_{0,i} \exp\left(\frac{-1}{\sigma_{0,i}^2}\right), \ \alpha_i = \frac{T_{s,i}}{\lambda_{0,i} + \beta_i},\tag{17}$$

where $T_{s,i}$ is the duration of the i-th sound file $\mathfrak{F}(\cdot)$. The equality constraints in (17) ensure that $c_i(\theta_u) = 0$ and $c_i(\theta_f) = T_{s,i}$. In other words, the nonlinear scaling functions are guaranteed to map the initial unfolded conformation to time instant 0 in the sound file and the final folded conformation to time instant $T_{s,i}$, which corresponds to the duration of the i-th sound file $\mathfrak{F}(\cdot)$.

The significance of the proposed sample-based wave space function in (15)–(17) is the generation of sounds from available recordings $_{\vec{A}}(\cdot)$ by scanning the scalar field $V_s(\cdot)$ along the data-driven conformation trajectories of protein molecules during the folding process. Each of the sound files $_{\vec{A}}(\cdot)$ are chosen arbitrarily and specific to the artistic flavor of the application at hand. For instance, they could be recorded by the sound designer in an ad-hoc



⁴https://cycling74.com/products/max

manner or as demonstrated in Section 5 sourced via other means (e.g., a piece of classical music). The nonlinear scaling functions $c_i(\cdot)$ in (16), $1 \le i \le 2N$, based on which the data-driven audio signal sampling is performed, guide the scanning process of the scalar field $V_s(\cdot)$ using the molecule conformations during folding.

Remark 8 (Comparison with the Original Sample-Based WSS) In Hermann's original work [28], the static sample-based wave space functions utilize linear scaling mappings of the form $c_i(\theta) = c_i \cdot \theta_i$, $1 \le i \le 2N$. In this article, we are introducing a new type of nonlinear scaling functions depending on designated conformations of protein molecules, namely, the folded θ_f and the unfolded θ_u conformations. From this perspective, our proposed sample-based wave space function in (15)–(17) can also be considered as a hybrid of Hermann's static sampling-based method (because of relying on recorded sound signals) and of Hermann's data-driven localized method (because of dependency on designated points in a given dataset).

Remark 9 (Computer-Generated Portamento) A natural way for instruments with continuously variable pitch like violin or human voice to make transitions between two musical notes is called portamento. Henderson and Solomon [26] have recently demonstrated that using one-dimensional optimal transport numerical algorithms it is possible to achieve computer-generated portamento. An interesting potential for the sample-based WSS function in (15), although not explored in this paper, is achieving portamento for transitioning between two musical notes, where the initial musical note is associated with a given designated protein conformation (e.g., an unfolded conformation) and the target musical note is associated with a target/final designated protein conformation (e.g., a folded conformation).

5 Example

In this section we present the results associated with our proposed sonification methodology applied to a peptide backbone chain with a dihedral angle space of dimension 82. All of the numerical implementation has been carried out in MATLAB R2018b by utilizing the PROTOFOLD I framework [35, 54] on an Intel[®] CoreTM i7-6770HQ CPU@2.60GHz. Figure 4 depicts the folding process resulting from our numerical simulations.

As expected from the KCM-based folding iteration the molecule aggregated free energy converges to a local minimum located on the folding energy landscape (see [35, 55] for further details). Furthermore, as can be seen from Fig. 4a, the protein molecule conformation converges to a helix from its unfolded initial configuration. We are interested in generating non-speech auditory representation of this process according to the problem statement in Section 4. Finally, Fig. 4b depicts two sample projected folding pathway curves with the red and green diamonds corresponding to the unfolded and folded conformations, respectively. Indeed, these two three-dimensional curves are the projections of the original folding pathway, which is embedded in a configuration space of dimension 82.

Canonical WSS We apply the canonical wave space sonification method proposed in Section 4.1 to the folding pathway dataset associated with the protein backbone peptide chain whose folding process is depicted in Fig. 4.

The five sound signals¹ generated by the proposed canonical wave space function in (12), (13) are depicted in Fig. 5. The base frequency in all these canonical wave space functions is chosen to be $f_0 = 250$ Hz. Furthermore, the duration of the sound files, which



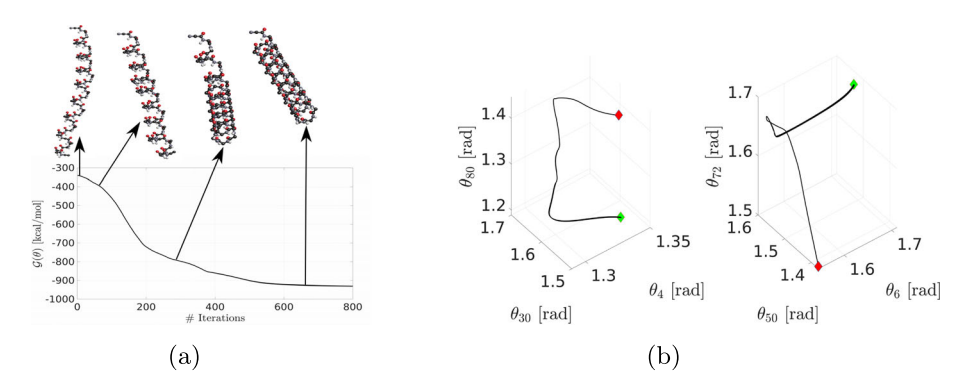


Fig. 4 The folding process of a protein peptide backbone chain with 82 DOFs: (a) the free energy of the molecule with its corresponding conformations along the folding pathway; and, (b) two sample 3D curves obtained by projecting the protein folding pathway on lower-dimensional spaces with the red and green diamonds corresponding to the unfolded and folded conformations, respectively

is a tunable parameter, is selected as $T_s = 5$ seconds. Moreover, the design parameters σ_0 for generating these sounds signals (see (13)) are chosen to be $\sigma_0 = 0.1$, $\sigma_0 = 0.15$, $\sigma_0 = 0.2$, $\sigma_0 = 0.3$, and $\sigma_0 = 0.4$, respectively. Finally, the parameter A_0 is set equal to 1 in all these sound signals.

The sepctrograms of the five sound signals¹ generated by the proposed canonical wave space function are depicted in Fig. 6. As expected from our sonification design methodology, while the conformation of the protein molecule approaches its final folded state, the frequency of the generated sound by the scalar field $V_{\circ}(\cdot)$ in (12) increases according to the frequency weighting function given by (13).

Sample-based WSS We apply the sample-based wave space sonification method proposed in Section 4.2 to the folding pathway dataset whose folding process is depicted in Fig. 4.

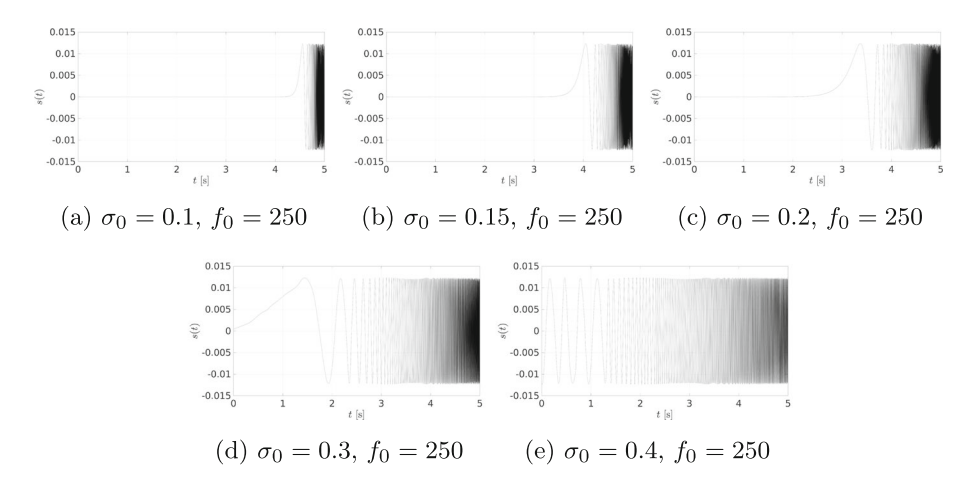


Fig. 5 The sound signals generated by the proposed canonical wave space function in (12) applied to a protein backbone peptide chain with 82 DOFs. As the conformation of the protein molecule approaches its final folded state, the frequency of the generated sound increases. The generated sound files (in .wav format) can be downloaded from https://dralirezamoha.github.io/proteinpathway/wssFoldingSoundFiles.zip



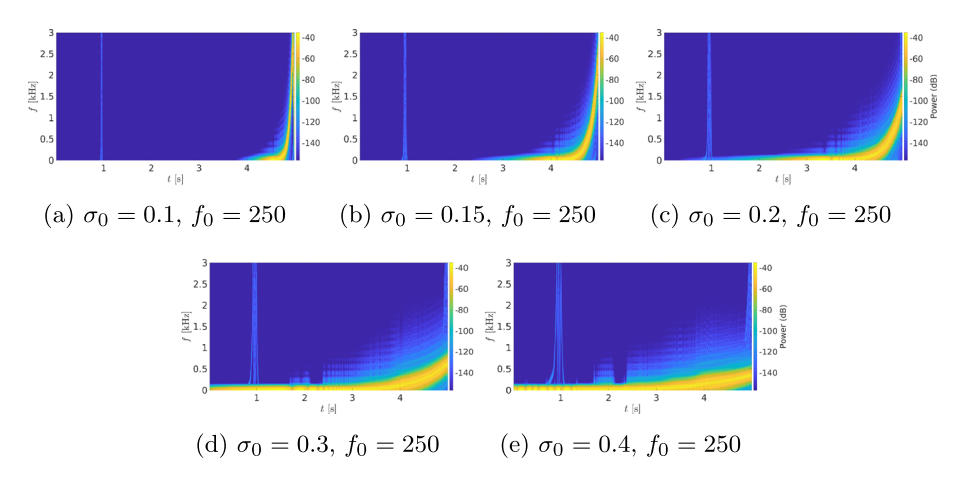


Fig. 6 The sepctrograms of the sound signals generated by the proposed canonical wave space function in (12) applied to a protein backbone peptide chain with 82 DOFs. As the conformation of the protein molecule approaches its final folded state, the frequency of the generated sound increases

We have chosen a piece of Mozart's Alla Turca for applying our sample-based WSS method to. This piece has been performed by Walter Gieseking and is available from his "Historic Broadcast Performances (1944–1950)" collection [45]. The original sound signal $\mathscr{M}(\cdot)$ and its spectrogram are depicted in Fig. 7.

To determine the sample-based wave space function given by (15)–(17), we need to determine the sound files $\sigma(\cdot)$ and the scaling functions $\sigma(\cdot)$. We have chosen all the sound files to be given by $\sigma(\cdot) = \sigma(\cdot)$, where $\sigma(\cdot)$ is the piece of Mozart's Alla Turca demonstrated in Fig. 7. Furthermore, we have chosen all the tuning parameters $\sigma(\cdot)$ and $\sigma(\cdot)$ to be the same for the nonlinear scaling functions, which results in $\sigma(\cdot) = \sigma(\cdot)$, $\sigma(\cdot) = \sigma(\cdot)$, $\sigma(\cdot) = \sigma(\cdot)$ and $\sigma(\cdot) = \sigma(\cdot)$ where $\sigma(\cdot) = \sigma(\cdot)$ are $\sigma(\cdot) = \sigma(\cdot)$ and $\sigma(\cdot) = \sigma(\cdot)$ and $\sigma(\cdot) = \sigma(\cdot)$ are $\sigma(\cdot) = \sigma(\cdot)$.

Figure 8 depicts the result of applying our sample-based WSS method to the chosen piece of Mozart's Alla Turca. The resulting sound signals¹ and the nonlinear scaling function $c_0(\cdot)$ along the protein folding pathway are demonstrated in the figure. In all the plots in Fig. 8, the parameter λ_0 is chosen to be equal to 1. We have chosen three different values

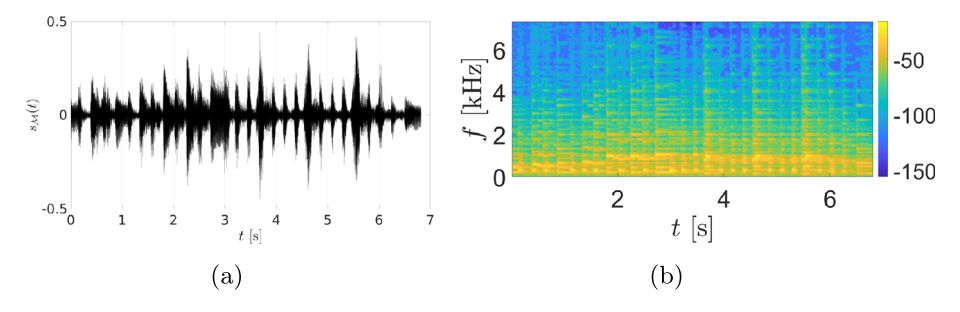


Fig. 7 The music piece taken from Mozart's Alla Turca: (a) the original sound signal; and, (b) the spectrogram associated with the sound signal



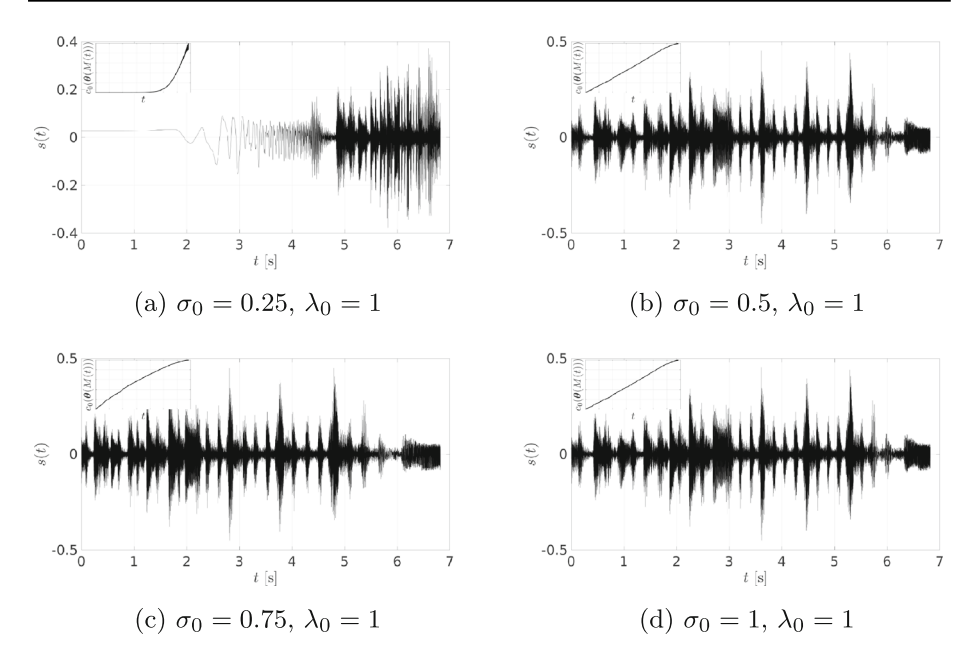


Fig. 8 The sound signals generated by the proposed sample-based wave space function in (15)–(17) with sound samples taken from Mozart's All Turca [45] applied to a protein backbone peptide chain with 82 DOFs. The embedded smaller plots demonstrate how the nonlinear scaling function $c_0(\cdot)$ varies along the protein folding pathway. The generated sound files (in .wav format) can be downloaded from https://dralirezamoha.github.io/proteinpathway/wssFoldingSoundFiles.zip

for σ_0 , namely, 0.25, 0.5, 0.75, and 1. The sepctrograms of the sound signals generated by the proposed sample-based wave space function are depicted in Fig. 9.

In the beginning, when the conformation of the peptide chain is far away from the final folded conformation, the scaling function $c_0(\cdot)$ varies very slowly resulting in sound patterns not familiar to the ear. This is specifically evident in the case of $\sigma_0=0.25$ and $\sigma_0=0.5$. This unnatural sound corresponds to the low frequency content of the generated sound as demonstrated by the spectrograms in Fig. 9. As the peptide chain starts approaching its final folded conformation, the heard sound begins taking the familiar form of Mozart's All Turca. In other words, the listener hears a sound file that gradually takes a familiar auditory form as the protein backbone peptide chain approaches its final folded conformation. The transition to a familiar sound and emergence of an ordered music pattern also corresponds to the protein configurational entropy loss while the molecule converges to its native folded state (see, e.g., [4] for further details on entropy loss during protein folding).

6 Discussion, concluding remarks, and future research directions

Discussion on the application of the proposed sonification method to other hyperredundant robotic mechanisms As discussed in Section 3, the KCM-based folding framework relies on describing the motion of protein molecules by modeling them as hyperredundant robotic mechanisms consisting of numerous rigid nano-linkages that fold under the nonlinear effect of the protein molecule interatomic forces. The justification for such a modeling approach is the experimental observations verifying that the the six atoms



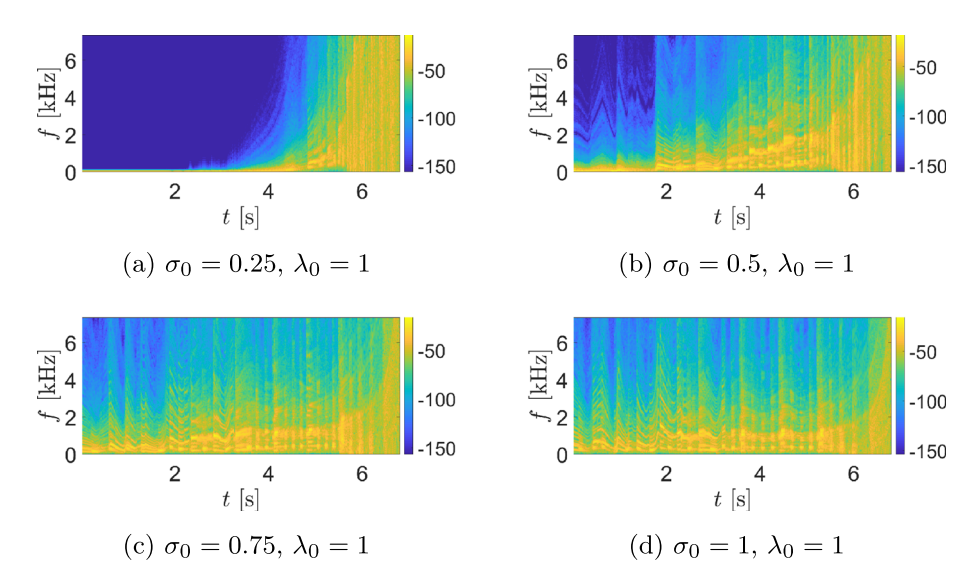


Fig. 9 The sepctrograms of the sound signals generated by the proposed sample-based wave space function in (15)–(17) with sound samples taken from Mozart's All Turca [45] applied to a protein backbone peptide chain with 82 DOFs

 C_{α} – CO – NH – C_{α} are coplanar in each of the protein peptide planes (see Fig. 2). Another notable fact is that each alpha-Carbon atom acts as a 2 DOF revolute joint playing the role of hinges in the kinematic mechanism.

Modeling the peptide planes as rigid links and treating the alpha-Carbon atoms as revolute joints have been the basis for various robotics-inspired approaches in the literature that model protein molecules as hyper-redundant mechanisms. For instance, the robotic kinematics-based point of view on the structure of proteins can be seen in the line of work by Kavraki and collaborators (see, e.g., [25, 56]), and Kazerounian and collaborators (see, e.g., [36, 55]), to name a few. Another interesting fact is that the protein kinematic model described in Section 3.1 has the exact same kinematic structure as robotic manipulators with hyper degrees-of-freedom as described in the work of Mochiyama et al. (see, e.g., [42]). This type of kinematic modeling has also been used for multisection continuum robots (see, e.g., [33]). Indeed, considering a hyper-redundant robotic mechanism with configuration vector $\theta \in \mathcal{Q}$, where \mathcal{Q} is a manifold of dimension N_0 , the time-indexed configuration vector $\theta(t) \in \mathcal{Q}$ represents the joint time profile trajectories of the hyper-redundant robot. Therefore, the same problem statement presented in Section 4 can also be considered for such robots. The only difference with the protein folding setting presented in this paper is the choice of designated configurations in the joint space of the robot. These designated configurations given by θ^* , instead of θ_u and θ_f in the case of protein molecules, can be generated by proper trajectory planning and obstacle avoidance algorithms designed for these hyper-redundant robotic mechanisms (see, e.g., [40]).

Concluding remarks and future research directions In this paper we proposed a WSS-based solution to the problem of sonification of protein folding pathway datasets. By utilizing the powerful WSS framework, we developed a systematic way of generating sounds from the dihedral angle folding trajectories of protein molecules, which are modeled as hyper-redundant robotic mechanisms with many rigid nano-linkages. As an example, we



applied the developed sonification methodology to the backbone chain of a protein molecule with a dihedral angle space of dimension 82. Specifically, a canonical wave space function based on a sum-of-sinusoids with conformation-dependent frequencies and a sample-based wave space function based on Mozart's Alla Turca are utilized for the sonification of the folding trajectories of this peptide chain. As future research directions, we envision extending the proposed sonification methodology in this paper to solving the sonification problem for the motion of soft robots and industrial collaborative multi-robot systems, where the robotic system operation generates an overwhelming amount of data.

Acknowledgments This work is supported by the National Science Foundation (NSF) through the award number CMMI-2153744.

Data Availability Statement The datasets codes generated during and/or analysed during the current study are available in the GitHub repository, https://dralirezamoha.github.io/proteinpathway/wssFoldingSoundFiles.zip, https://dralirezamoha.github.io/proteinpathway/2023MTAP_Canonical_WaveSpaceSonification.zip, and https://dralirezamoha.github.io/proteinpathway/2023MTAP_MatlabFiles_SampleBasedWSS.zip.

Declarations

Conflict of Interests The authors declare that they have no conflict of interest.

References

- Adolf DB, Ediger MD (1991) Brownian dynamics simulations of local motions in polyisoprene. Macromolecules 24(21):5834–5842
- 2. Alvarado C, Kazerounian K (2003) On the rotational operators in protein structure simulations. Protein Eng 16(10):717–720
- 3. Arkun Y, Erman B (2010) Prediction of optimal folding routes of proteins that satisfy the principle of lowest entropy loss: dynamic contact maps and optimal control. PloS One 5(10):e13275
- Arkun Y, G

 ür M (2012) Combining optimal control theory and molecular dynamics for protein folding. PLoS One 7(1):e29628
- 5. Barrass S, Kramer G (1999) Using sonification. Multimedia Syst 7(1):23-31
- Behandish M, Tavousi P, Ilieş HT, Kazerounian K (2013) GPU-accelerated computation of solvation free energy for kinetostatic protein folding simulation. In: ASME International design engineering technical conferences and computers and information in engineering conference, vol 55850. American Society of Mechanical Engineers, pp 02–02009
- Bergasa-Caceres F, Rabitz HA (2020) Interdiction of protein folding for therapeutic drug development in SARS CoV-2. J Phys Chem B 124(38):8201–8208
- 8. Brazil E, Fernström M (2011) Auditory icons. In: Hermann T, Hunt A, Neuhoff JG (eds) The sonification handbook. Logos Verlag, Berlin
- 9. Bremner P, Mitchell TJ, McIntosh V (2022) The impact of data sonification in virtual reality robot teleoperation. Front Virt Real 3:904720
- 10. Bresin R, Frid E, Latupeirissa A, Panariello C (2021) Robust non-verbal expression in humanoid robots: new methods for augmenting expressive movements with sound. In: Workshop on sound in human-robot interaction, ACM/IEEE international conference on human-robot interaction
- Cabral JP, Remijn GB (2019) Auditory icons: design and physical characteristics. Appl Ergon 78:224– 239
- Chorsi MT, Tavousi P, Mundrane C, Gorbatyuk V, Ilieş H, Kazerounian K (2020) One degree of freedom 7-R closed loop linkage as a building block of nanorobots. In: International symposium on advances in robot kinematics. Springer, pp 41–48
- Delatour T (2000) Molecular music: the acoustic conversion of molecular vibrational spectra. Comput Music J 24(3):48–68
- 14. Dunn J, Clark MA (1999) Life music: the sonification of proteins. Leonardo 32(1):25-32
- Errede S (2017) Lecture notes in acoustical physics of music. University of Illinois Urbana-Champaign (UIUC)



- Feng Z, Hu G, Sun Y, Soon J (2020) An overview of collaborative robotic manipulation in multi-robot systems. Annu Rev Control 49:113–127
- 17. Ferina J, Daggett V (2019) Visualizing protein folding and unfolding. J Mol Biol 431(8):1540-1564
- 18. Finkelstein AV, Ptitsyn O (2016) Protein physics: a course of lectures. Amsterdam, The Netherlands; Boston, MA, USA; Heidelberg, Germany; London, UK; New York, NY, USA; Oxford, UK; Paris, France; San Diego, CA, USA; Singapore; Sydney, Australia; Tokyo, Japan
- 19. Franjou SL, Milazzo M, Yu C-H, Buehler MJ (2019) Sounds interesting: can sonification help us design new proteins? Expert Rev Proteomics 16(11–12):875–879
- Franjou SL, Milazzo M, Yu C-H, Buehler MJ (2021) A perspective on musical representations of folded protein nanostructures. Nano Futures 5(1):012501
- Frid E, Bresin R (2022) Perceptual evaluation of blended sonification of mechanical robot sounds produced by emotionally expressive gestures: augmenting consequential sounds to improve non-verbal robot communication. Int J Soc Robot 14(2):357–372
- Frid E, Bresin R, Alexanderson S (2018) Perception of mechanical sounds inherent to expressive gestures
 of a Nao robot-implications for movement sonification of humanoids. In: Proceedings of the sound and
 music computing conference (SMC), pp 53–59
- Fryman J, Matthias B (2012) Safety of industrial robots: from conventional to collaborative applications.
 In: ROBOTIK 2012; 7th German conference on robotics. VDE, pp 1–5
- George Thuruthel T, Ansari Y, Falotico E, Laschi C (2018) Control strategies for soft robotic manipulators: a survey. Soft Rob 5(2):149–163
- Haspel N, Moll M, Baker ML, Chiu W, Kavraki LE (2010) Tracing conformational changes in proteins. BMC Struct Biol 10(1):1–11
- 26. Henderson T, Solomon J (2019) Audio transport: a generalized portamento via optimal transport. In: The 22nd International conference on digital audio effects (DAFx-19), Birmingham
- 27. Hermann T (2008) Taxonomy and definitions for sonification and auditory display. In: Proceedings of the 14th international conference on auditory display (ICAD), Pari
- 28. Hermann T (2018) Wave space sonification. In: Proceedings of the 24th international conference on auditory display (ICAD). Michigan Technological University, Houghton
- Hermann T, Ritter H (1999) Listen to your data: model-based sonification for data analysis. Advances in Intelligent Computing and Multimedia Systems
- 30. Hermann T, Ritter H (2005) Model-based sonification revisited—authors' comments on hermann and ritter, icad 2002. ACM Trans Appl Percept (TAP) 2(4):559–563
- 31. Hermann T, Hunt A, Neuhoff JG (2011) The sonification handbook. Logos Verlag, Berlin
- 32. Hu Z, Yuan H, Xu W, Yang T, Liang B (2021) Equivalent kinematics and pose-configuration planning of segmented hyper-redundant space manipulators. Acta Astronaut 185:102–116
- Jones BA, Walker ID (2006) Kinematics for multisection continuum robots. IEEE Trans Rob 22(1):43–
- Kalonaris S, Zannos I (2021) High-order surrogacy for the audiovisual display of dance. In: Proceedings of the 26th international conference on auditory display (ICAD), Virtual
- Kazerounian K, Latif K, Alvarado C (2005) PROTOFOLD: a successive kinetostatic compliance method for protein conformation prediction. J Mech Des 127(4):712–717
- Kazerounian K, Latif K, Rodriguez K, Alvarado C (2005) Nano-kinematics for analysis of protein molecules. J Mech Des 127(4):699–711
- Lazzarini V, Yi S, Heintz J, Brandtsegg O, McCurdy I et al (2016) Csound: a sound and music computing system. Springer, Cham
- Lemkul JA (2018) From proteins to perturbed Hamiltonians: a suite of tutorials for the gromacs-2018 molecular simulation package [article v1.0]. Living J Comput Molecul Sci 1(1):5068. https://doi.org/10.33011/livecoms.1.1.5068
- 39. Madden C, Bohnenkamp P, Kazerounian K, Ilieş HT (2009) Residue level three-dimensional workspace maps for conformational trajectory planning of proteins. Int J Robot Res 28(4):450–463
- Menon MS, Ravi VC, Ghosal A (2017) Trajectory planning and obstacle avoidance for hyper-redundant serial robots. J Mech Robot 9:4
- Michael E, Simonson T (2022) How much can physics do for protein design? Curr Opin Struct Biol 72:46–54
- Mochiyama H, Shimemura E, Kobayashi H (1999) Shape control of manipulators with hyper degrees of freedom. Int J Robot Res 18(6):584–600
- Mohammadi A, Spong MW (2021) Quadratic optimization-based nonlinear control for protein conformation prediction. IEEE Control Syst Lett 6:373–378
- Mohammadi A, Spong MW (2022) Chetaev instability framework for kinetostatic compliance-based protein unfolding. IEEE Control Syst Lett 6:2755–2760



- Mozart WA (1783) Piano sonata no. 11 in a major, k. 331: Iii. rondo alla turca: Allegretto, Salzburg. Album: Walter Gieseking: Historic Broadcast Performances (1944–1950)
- Mundrane C, Chorsi M, Vinogradova O, Ilieş H, Kazerounian K (2022) Exploring electric field perturbations as the actuator for nanorobots and nanomachines. In: International symposium on advances in robot kinematics. Springer, pp 257–265
- 47. Neuhoff JG, Kramer G, Wayand J (2000) Sonification and the interaction of perceptual dimensions: can the data get lost in the map? In: Proceedings of the 6th international conference on auditory display (ICAD), Atlanta
- 48. Nown TH, Upadhyay P, Kerr A, Andonovic I, Tachtatzis C, Grealy MA (2022) A mapping review of real-time movement sonification systems for movement rehabilitation. IEEE Rev Biomed Eng
- 49. Qin Z, Buehler MJ (2019) Analysis of the vibrational and sound spectrum of over 100,000 protein structures and application in sonification. Extreme Mech Lett 29:100460
- Schwenk M, Arras KO (2014) R2-D2 reloaded: a flexible sound synthesis system for sonic humanrobot interaction design. In: The 23rd IEEE international symposium on robot and human interactive communication, pp 161–167
- Shahbazi Z, Ilieş HT, Kazerounian K (2010) Hydrogen bonds and kinematic mobility of protein molecules. J Mech Robot 2(2):021009
- Shoemaker BA, Wang J, Wolynes PG (1997) Structural correlations in protein folding funnels. Proc Natl Acad Sci 94(3):777–782
- Subramanian R, Kazerounian K (2007) Kinematic mobility analysis of peptide based nano-linkages. Mech Mach Theory 42(8):903–918
- Tavousi P (2016) On the systematic design and analysis of artificial molecular machines. Ph.D. Thesis, University of Connecticut
- 55. Tavousi P, Behandish M, Ilieş HT, Kazerounian K (2015) Protofold II: enhanced model and implementation for kinetostatic protein folding. ASME J Nanotechnol Eng Med 6:3
- Teodoro ML, Phillips GN, Kavraki LE (2001) Molecular docking: a problem with thousands of degrees of freedom. In: Proceedings of 2001 IEEE international conference on robotics and automation (ICRA), vol 1. IEEE, pp 960–965
- Thagard P (2012) Creative combination of representations: scientific discovery and technological invention. Psychology of science: Implicit and explicit processes, 389–405
- 58. Triantafyllidis E, Mcgreavy C, Gu J, Li Z (2020) Study of multimodal interfaces and the improvements on teleoperation. IEEE Access 8:78213–78227
- Trivedi D, Rahn CD, Kier WM, Walker ID (2008) Soft robotics: biological inspiration, state of the art, and future research. Appl Bion Biomech 5(3):99–117
- Yu C-H, Buehler MJ (2020) Sonification based de novo protein design using artificial intelligence, structure prediction, and analysis using molecular modeling. APL Bioeng 4(1):016108
- Yu C-H, Qin Z, Martin-Martinez FJ, Buehler MJ (2019) A self-consistent sonification method to translate amino acid sequences into musical compositions and application in protein design using artificial intelligence. ACS Nano 13(7):7471–7482
- Zbiss K, Kacem A, Santillo M, Mohammadi A (2022) Automatic collision-free trajectory generation for collaborative robotic car-painting. IEEE Access 10:9950–9959
- Zhang BJ, Sigafoos N, Moffit R, Syed I, Adams LS, Fick J, Fitter NT (2022) Sonifyit: towards transformative sound for all robots. IEEE Robot Autom Lett 7(4):10566–10572
- Zhao Y, Jin L, Zhang P, Li J (2018) Inverse displacement analysis of a hyper-redundant elephant's trunk robot. J Bionic Eng 15(2):397–407

Publisher's note Springer Nature remains neutral with regard to jurisdictional claims in published maps and institutional affiliations.

Springer Nature or its licensor (e.g. a society or other partner) holds exclusive rights to this article under a publishing agreement with the author(s) or other rightsholder(s); author self-archiving of the accepted manuscript version of this article is solely governed by the terms of such publishing agreement and applicable law.

